Enzyme Models

DOI: 10.1002/anie.200900118

Structural Characterization and Remarkable Axial Ligand Effect on the Nucleophilic Reactivity of a Nonheme Manganese(III)–Peroxo Complex**

Jamespandi Annaraj, Jaeheung Cho, Yong-Min Lee, Sung Yeon Kim, Reza Latifi, Sam P. de Visser, and Wonwoo Nam**

Manganese(III) peroxo complexes are postulated as reactive intermediates in the reactions of Mn-containing enzymes such as manganese superoxide dismutase (Mn-SOD), catalase, and the oxygen-evolving complex (OEC) of photosystem II.[1] In biomimetic studies, a number of manganese(III)–O_2 complexes have been synthesized and characterized with various spectroscopic techniques.[2] X-ray crystal structures of heme and nonheme Mn^{III}–peroxo complexes were also reported, such as a side-on peroxo manganese(III) porphyrin complex $[Mn^{III}(TPP)(O_2)]^-$ (TPP = *meso*-tetraphenylporphyrin)[3] and two monomeric side-on peroxo manganese(III) complexes bearing nonheme ligands.[2c,d] The manganese(III)–peroxo complexes have shown reactivity in oxidative nucleophilic reactions with substrates such as acyl halides, aldehydes, and electron-deficient olefins.[2c,4,5]

Axial ligands play key roles in dioxygen activation by metalloenzymes and model compounds.[6] For example, reactivities of high-valent iron–oxo intermediates in heme enzymes and iron porphyrin models are markedly affected by axial ligands *trans* to the iron–oxo group in electrophilic oxidation reactions.[7] Very recently, the axial ligand effect was also demonstrated in electrophilic oxidation reactions by nonheme iron(IV) and ruthenium(IV) oxo complexes.[8] In contrast, the axial ligand effect has rarely been investigated in oxidative nucleophilic reactions of metal peroxo complexes.[9] Herein, we report the synthesis and X-ray crystal structure of a manganese(III)–peroxo complex bearing a 13-membered macrocyclic ligand, $[Mn^{III}(13\text{-TMC})(O_2)]^+$ (**1**; 13-TMC = 1,4,7,10-tetramethyl-1,4,7,10-tetraazacyclotridecane). The X-ray crystal structure of **1** shows the binding of a peroxo ligand in a side-on η^2 fashion. We also report for the first time a remarkable axial ligand effect on the reactivity of the Mn^{III}–peroxo complex in oxidative nucleophilic reactions.

Addition of five equivalents H_2O_2 to a solution containing $[Mn(13\text{-TMC})](CF_3SO_3)_2$ and 2.5 equivalents triethylamine (TEA) in CH_3CN at 10 °C afforded a green intermediate **1** with absorption bands at 288 ($\varepsilon = 2440\,M^{-1}cm^{-1}$), 452 ($\varepsilon = 390\,M^{-1}cm^{-1}$), and 615 nm ($\varepsilon = 190\,M^{-1}cm^{-1}$; see the Supporting Information, Figure S1a). The intermediate persisted for several days at 25 °C. The electrospray ionization mass spectrum (ESI-MS) of **1** exhibits a prominent ion peak at a mass-to-charge ratio (m/z) of 329.1 (Supporting Information, Figure S1b), whose mass and isotope distribution pattern correspond to $[Mn(13\text{-TMC})(O_2)]^+$ (calculated m/z 329.2). When the reaction was carried out with isotopically labeled $H_2{}^{18}O_2$, a mass peak corresponding to $[Mn(13\text{-TMC})(^{18}O_2)]^+$ appeared at m/z 333.1. The shift of four mass units upon the substitution of ^{16}O with ^{18}O indicates that **1** contains an O_2 unit. The X-band EPR spectrum of **1** is silent, suggesting that **1** is either a high-spin ($S = 2$) or intermediate-spin ($S = 1$) d^4 species. The spin state of **1** in CH_3CN solution was determined using the ^1H NMR spectroscopy method of Evans,[10] and the room-temperature magnetic moment of $5.5\,\mu_B$ clearly indicates a high-spin state ($S = 2$) of the Mn^{III} species.

Green platelike crystals were obtained upon addition of $NaBPh_4$ to a solution of **1** in CH_3CN at −40 °C, and a crystallographic analysis of the single crystals clearly established that **1** contains a monomeric six-coordinate Mn^{III} cation with a side-on peroxo ligand, $[Mn(13\text{-TMC})(O_2)]^+$ (Figure 1; Supporting Information Figure S2 and Tables S1 and S2). The O–O bond of 1.410(4) Å is typical for a peroxide ion bound to a transition-metal ion,[11] but it is slightly longer than that found in $[Mn(14\text{-TMC})(O_2)]^+$ (**2**, 14-TMC = 1,4,8,11-tetramethyl-1,4,8,11-tetraazacyclotetradecane, 1.403 Å).[2c] The peroxo group is quite symmetrically bound to the manganese ion in a side-on η^2 fashion with an average Mn–O bond length of 1.859 Å that is slightly shorter than that in **2** (1.884 Å). The nominally octahedral geometry of the Mn^{III} ion is very distorted owing to the triangular MnO_2 moiety with a small bite angle of 44.55(11)° (Supporting Information, Figure S2). All four *N*-methyl groups of the 13-TMC ligand point toward the peroxo ligand, as observed in the structure of **2**.[2c]

[*] Dr. J. Annaraj,[+] Prof. Dr. J. Cho,[+] Prof. Dr. Y.-M. Lee, S. Y. Kim, Prof. Dr. W. Nam
Department of Chemistry and Nano Science, Department of Bioinspired Science, and Center for Biomimetic Systems
Ewha Womans University
Seoul 120–750 (Korea)
Fax: (+82) 2-3277-4441
E-mail: wwnam@ewha.ac.kr
R. Latifi, Dr. S. P. de Visser
The Manchester Interdisciplinary Biocenter and the School of Chemical Engineering and Analytical Science
The University of Manchester
131 Princess Street, Manchester, M1 7DN (United Kingdom)
Fax: (+44) 161-306-5201
E-mail: sam.devisser@manchester.ac.uk
[+] These authors contributed equally to this work.

[**] The research was supported by KOSEF/MEST through the CRI Program and the WCU project (R31-2008-000-10010-0) (to W.N.) and by CPU time provided by the National Service of Computational Chemistry Software (to S.P. de V.).
Supporting information for this article is available on the WWW under http://dx.doi.org/10.1002/anie.200900118.

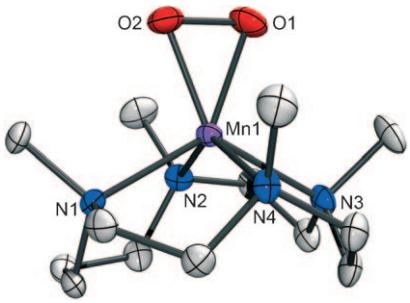

Figure 1. X-ray structure of the $[Mn^{III}(13\text{-TMC})(O_2)]^+$ cation (**1**) showing 30% probability thermal ellipsoids. Hydrogen atoms are omitted for clarity. Selected bond lengths [Å]: Mn1–O1 1.863(2), Mn1–O2 1.855(2), Mn1–N1 2.191(3), Mn1–N2 2.283(3), Mn1–N3 2.201(3), Mn1–N4 2.291(3), O1–O2 1.410(4).

We then investigated the nucleophilic character of **1** in aldehyde deformylation. There is precedent for the reaction of heme and nonheme metal(III) peroxo complexes with aldehydes to give the corresponding deformylated products.[2b,c,4,12] Upon addition of cyclohexanecarboxaldehyde (CCA) to **1** in CH_3CN, **1** disappeared with a first-order decay profile (Figure 2a). Pseudo-first-order fitting of the kinetic data allowed us to determine the rate constant to be $k_{obs} = 2.0(2) \times 10^{-3}\ s^{-1}$ at 10 °C (Figure 2a, inset). Product analysis of the resulting solution revealed the formation of cyclohexene and formate as products, as observed in the aldehyde deformylation of CCA by metal peroxo complexes including **2**.[2c,12c,13] The magnitude of the first-order rate constants increased proportionally with the aldehyde concentration, leading us to determine a second-order rate constant of $2.0(2) \times 10^{-2}\ M^{-1}\ s^{-1}$ at 10 °C (Figure 2c, blue line). It is worth noting that the reactivity of **1** is similar to that of **2** ($k_2 = 4.0 \times 10^{-2}\ M^{-1}\ s^{-1}$ at 10 °C) in the reaction with CCA under identical reaction conditions.

Interestingly, addition of NaN_3 (1.2 equiv) to the solution of **1** (0.5 mM) did not change the UV/Vis spectrum much (Figure 2a,b, blue line), but the intermediate disappeared rapidly upon the addition of CCA even at a lower temperature (e.g., −10 °C; Figure 2b). This result is of interest because **1** reacted slowly with CCA in the absence of NaN_3 at 10 °C (Figure 2a). We therefore decided to investigate the effect of axial ligands in nucleophilic reactions with **1**-X bearing different anionic ligands (X = N_3^- (**1**-N_3), $CF_3CO_2^-$ (**1**-OOCCF$_3$), NCS^- (**1**-NCS), and CN^- (**1**-CN)). First, **1**-X was prepared by adding either NaX or Bu_4NX to the solution of **1** (Scheme 1, route a) or by adding NaX or Bu_4NX to the solution of $[Mn(13\text{-TMC})](CF_3SO_3)_2$ and subsequently adding TEA and H_2O_2 to the resulting solution of $[Mn^{II}(13\text{-TMC})(X)]^+$ (Scheme 1, route b). In route b, the binding of X in $[Mn^{II}(13\text{-TMC})(X)]^+$ was confirmed by ESI-MS (Supporting Information, Figure S3), but the characterization of **1**-X by ESI-MS failed because the intermediates were neutral. Although the spectroscopic characterization of **1**-X for the binding of axial ligands was not successful, cyclic voltammetric measurements of **1**-X clearly demonstrate the binding of anionic ligands in the **1**-X series. First, the different redox potentials of the $[Mn^{II}(13\text{-TMC})(X)]^+$ complexes confirmed the binding of anionic ligands (Supporting Information,

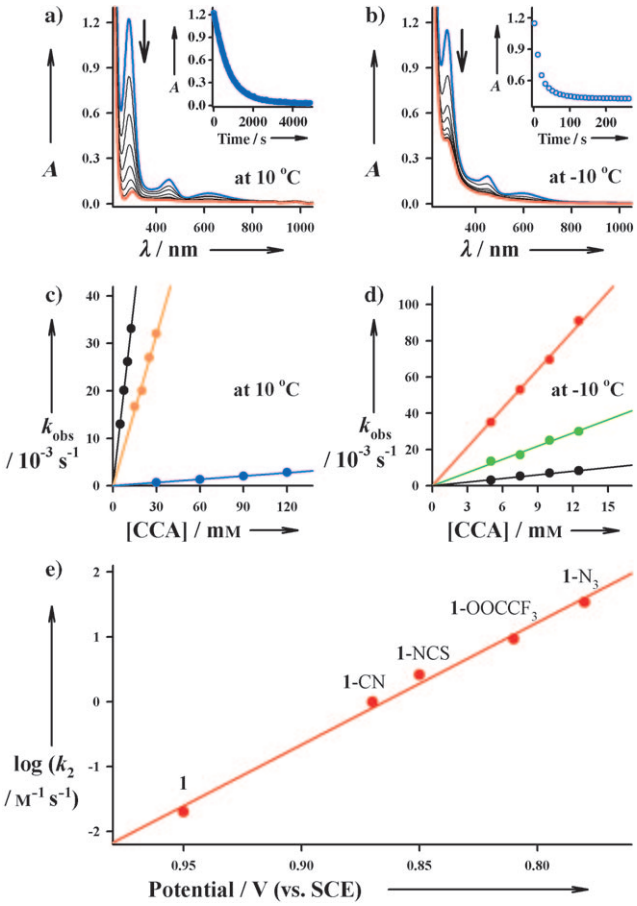

Figure 2. a) UV/Vis spectral changes of **1** (0.5 mM) upon addition of CCA (180 equiv, 90 mM). Inset shows the time course of the decay of **1** monitored at 288 nm. b) UV/Vis spectral changes of **1**-N_3 (0.5 mM) upon addition of CCA (10 equiv, 5 mM) at −10 °C. Inset shows the time course of the decay of **1**-N_3 monitored at 282 nm. c) Plots of k_{obs} against CCA concentration to determine second-order rate constants in the reactions of **1** (blue), **1**-CN (orange), and **1**-NCS (black) at 10 °C. d) Plots of k_{obs} against CCA concentration to determine second-order rate constants in the reactions of **1**-NCS (black), **1**-OOCCF$_3$ (green), and **1**-N_3 (red) at −10 °C. e) Plot of log k_2 of **1** and **1**-X at 10 °C against $E_{p,a}$ values of **1** and **1**-X. The k_2 values of **1**-OOCCF$_3$ and **1**-N_3 at 10 °C were calculated using the Eyring equation (see the Supporting Information, Figure S9 for detailed procedures).

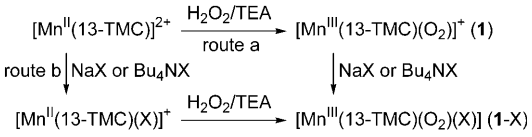

Scheme 1.

Figures S4 and S5), as evidenced by the ESI-MS data (Supporting Information, Figure S3). We then investigated the electrochemistry of **1** and observed a new oxidative wave with $E_{p,a} = 0.95$ V vs. SCE ($E_{p,a}$ = anodic peak potential, SCE = saturated calomel electrode; Supporting Information, Figure S5). This wave shifted in the negative direction upon binding of anionic ligands, affording $E_{p,a}$ values **1** (0.95 V) > **1**-CN (0.87 V) > **1**-NCS (0.85 V) > **1**-OOCCF$_3$ (0.82 V) >

1-N_3 (0.78 V; Supporting Information, Figures S6 and S7). Furthermore, the wave shifts in the positive direction when the scan rate is increased (Supporting Information, Figure S8). Thus, the different $E_{p,a}$ values of **1**-X clearly indicate the binding of anionic ligands. Moreover, on the basis of the observed $E_{p,a}$ values, the electron-richness of **1**-X is found to be in the order of **1**-N_3 > **1**-$OOCCF_3$ > **1**-NCS > **1**-CN > **1**, according to the electron-donating ability of the axial ligands $N_3^- > CF_3CO_2^- > NCS^- > CN^- > NCCH_3$.[8a]

The axial ligand effect on the reactivity of **1**-X was investigated in the deformylation of CCA by determining second-order rate constants of **1** ($k_2 = 2.0 \times 10^{-2}\,M^{-1}s^{-1}$), **1**-CN ($k_2 = 1.0\,M^{-1}s^{-1}$), and **1**-NCS ($k_2 = 2.6\,M^{-1}s^{-1}$) at 10 °C (Figure 2c) and **1**-NCS ($k_2 = 6.7 \times 10^{-1}M^{-1}s^{-1}$), **1**-$OOCCF_3$ ($k_2 = 2.4\,M^{-1}s^{-1}$), and **1**-N_3 ($k_2 = 7.1\,M^{-1}s^{-1}$) at −10 °C (Figure 2d). As the reactivity studies were performed at two different temperatures owing to the large reactivity difference within the **1**-X series, the k_2 values of **1**-$OOCCF_3$ and **1**-N_3 were normalized using the Eyring equation (Supporting Information, Figure S9) and used to plot reaction rates against the $E_{p,a}$ values of Mn^{III}–peroxo complexes (Figure 2e). The observed reactivity order of **1**-N_3 > **1**-$OOCCF_3$ > **1**-NCS > **1**-CN > **1** reflects an increase in the nucleophilicity of the $\{Mn^{III}O_2\}$ unit upon binding of anionic ligands that make the Mn^{III}–peroxo complex more electron-rich, as evidenced by the cyclic voltammetric data (see above). Furthermore, the nucleophilic character of the $\{Mn^{III}O_2\}$ unit was confirmed by carrying out reactions with *para*-substituted benzaldehydes bearing a series of electron-donating and -withdrawing substituents at the *para*-position of the phenyl group (*para*-Y-C_6H_4-CHO; Y = OMe, Me, F, H, Cl; Supporting Information, Figure S10), and with primary (1°-CHO), secondary (2°-CHO), and tertiary aldehydes (3°-CHO; Supporting Information, Figure S11). The observation of a positive ρ^+ value of 2.5 in the Hammett plot (Supporting Information, Figure S10) and the reactivity order of 1°-CHO > 2°-CHO > 3°-CHO (Supporting Information, Figure S11) are consistent with a process that depends on the nucleophilic character of the $\{Mn^{III}O_2\}$ unit in the oxidation of aldehydes. After completion of the reactions, we have confirmed that the anionic ligand X remains coordinated to the $\{Mn^{II}(TMC)\}$ unit by ESI MS of the resulting solutions (Supporting Information, Figure S12).

How, then, is the nucleophilicity of the Mn^{III}–peroxo complex affected by the introduction of anionic axial ligands *trans* to the peroxo group? Two factors are considered for the increased nucleophilicity of **1**-X: electronic and structural effects. First, the electronic effect is that binding of an electron-donating anionic axial ligand makes the Mn^{III}–peroxo complex more electron-rich,[14] resulting in an increase of the nucleophilicity of the peroxo group. We have shown in the electrochemical investigation that the binding of anionic ligands shifts the redox potentials of **1**-X negatively (Supporting Information, Figure S6), thus indicating that **1**-X becomes more electron-rich by binding anionic axial ligands. We have also observed a good linear correlation between the $E_{p,a}$ values of **1**-X and the reaction rates of CCA oxidation by the intermediates (Figure 2e), thus demonstrating that the Mn^{III}–peroxo complexes with more electron-donating axial ligands are more reactive in oxidative nucleophilic reactions. Thus, the reactivity order of **1**-N_3 > **1**-$OOCCF_3$ > **1**-NCS > **1**-CN > **1** follows the electron-richness of **1**-N_3 > **1**-$OOCCF_3$ > **1**-NCS > **1**-CN > **1** in nucleophilic reactions.

The structural effect is that binding of an axial ligand *trans* to the peroxo group may facilitate the conversion of the side-on peroxo ligand into an end-on peroxo ligand, thus making it more nucleophilic (Scheme 2).[9] That is, upon binding, the axial ligand pulls the metal ion down into the coordination plane of the 13-TMC ligand, as in heme systems (Scheme 2, **A**).[15] As a consequence, the peroxo group experiences more repulsive interactions from atoms in the 13-TMC ring, resulting in the shift of the equilibrium toward the end-on conformation (Scheme 2, **B**). Preliminary DFT calculations on the side-on and end-on Mn^{III}–peroxo complexes indicate that the peroxo group in the end-on structure has much more anionic character than that in the side-on structure; the electron densities at the oxygen atoms in the end-on and side-on peroxo groups are −0.63 and −0.24, respectively (Supporting Information, Tables S3 and S4 and Figure S13). Therefore, the oxygen atom in the end-on structure will be more likely to react by nucleophilic oxidation reactions than that in the side-on structure.

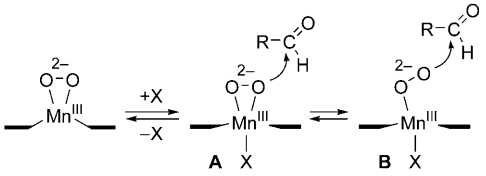

Scheme 2.

In conclusion, we have reported the crystal structure of a nonheme Mn^{III}–peroxo complex in which the peroxo ligand is bound in a side-on η^2 fashion. We have also shown that the nucleophilicity of the Mn^{III}–peroxo complex is markedly increased by the introduction of anionic axial ligands *trans* to the peroxo group. The increased nucleophilicity is interpreted by considering the electronic and structural changes of the Mn^{III}–peroxo complex upon binding axial ligands, such as the increased electron-richness and a change from a side-on to an end-on conformation of the peroxo group.

Received: January 8, 2009
Revised: February 20, 2009
Published online: May 7, 2009

Keywords: axial ligand effects · bioinorganic chemistry · enzyme models · manganese · nucleophilic reactions

[1] a) K. Barnese, E. B. Gralla, D. E. Cabelli, J. S. Valentine, *J. Am. Chem. Soc.* **2008**, *130*, 4604–4606; b) R. Tagore, H. Chen, R. H. Crabtree, G. W. Brudvig, *J. Am. Chem. Soc.* **2006**, *128*, 9457–9465, and references therein; c) A. J. Wu, J. E. Penner-Hahn, V. L. Pecoraro, *Chem. Rev.* **2004**, *104*, 903–938.

[2] a) S. Groni, P. Dorlet, G. Blain, S. Bourcier, R. Guillot, E. Anxolabéhère-Mallart, *Inorg. Chem.* **2008**, *47*, 3166–3172; b) R. L. Shook, W. A. Gunderson, J. Greaves, J. W. Ziller, M. P.

Hendrich, A. S. Borovik, *J. Am. Chem. Soc.* **2008**, *130*, 8888 – 8889; c) M. S. Seo, J. Y. Kim, J. Annaraj, Y. Kim, Y.-M. Lee, S.-J. Kim, J. Kim, W. Nam, *Angew. Chem.* **2007**, *119*, 381 – 384; *Angew. Chem. Int. Ed.* **2007**, *46*, 377 – 380; d) N. Kitajima, H. Komatsuzaki, S. Hikichi, M. Osawa, Y. Moro-Oka, *J. Am. Chem. Soc.* **1994**, *116*, 11596 – 11597.

[3] R. B. VanAtta, C. E. Strouse, L. K. Hanson, J. S. Valentine, *J. Am. Chem. Soc.* **1987**, *109*, 1425 – 1434.

[4] D. L. Wertz, J. S. Valentine, *Struct. Bonding (Berlin)* **2000**, *97*, 37 – 60.

[5] a) M. F. Sisemore, M. Selke, J. N. Burstyn, J. S. Valentine, *Inorg. Chem.* **1997**, *36*, 979 – 984; b) J. T. Groves, Y. Watanabe, T. J. McMurry, *J. Am. Chem. Soc.* **1983**, *105*, 4489 – 4490.

[6] a) J. A. Kovacs, L. M. Brines, *Acc. Chem. Res.* **2007**, *40*, 501 – 509; b) W. Nam, *Acc. Chem. Res.* **2007**, *40*, 522 – 531.

[7] a) J. H. Dawson, *Science* **1988**, *240*, 433 – 439; b) M. T. Green, J. H. Dawson, H. B. Gray, *Science* **2004**, *304*, 1653 – 1656; c) Z. Gross, S. Nimri, *Inorg. Chem.* **1994**, *33*, 1731 – 1732; d) W. J. Song, Y. O. Ryu, R. Song, W. Nam, *J. Biol. Inorg. Chem.* **2005**, *10*, 294 – 304.

[8] a) C. V. Sastri, J. Lee, K. Oh, Y. J. Lee, J. Lee, T. A. Jackson, K. Ray, H. Hirao, W. Shin, J. A. Halfen, J. Kim, L. Que, Jr., S. Shaik, W. Nam, *Proc. Natl. Acad. Sci. USA* **2007**, *104*, 19181 – 19186; b) H. Hirao, L. Que, Jr., W. Nam, S. Shaik, *Chem. Eur. J.* **2008**, *14*, 1740 – 1756; c) S. N. Dhuri, M. S. Seo, Y.-M. Lee, H. Hirao, Y. Wang, W. Nam, S. Shaik, *Angew. Chem.* **2008**, *120*, 3404 – 3407; *Angew. Chem. Int. Ed.* **2008**, *47*, 3356 – 3359.

[9] It has been reported by Selke and Valentine that binding of a solvent molecule as an axial ligand (e.g., DMSO) increases the nucleophilic reactivity of a ferric peroxo porphyrin complex in the epoxidation of electron-deficient olefins. The authors proposed that axial ligands push the side-on-binding peroxo group open and make the peroxo ligand more nucleophilic. See M. Selke, J. S. Valentine, *J. Am. Chem. Soc.* **1998**, *120*, 2652 – 2653.

[10] D. F. Evans, D. A. Jakubovic, *J. Chem. Soc. Dalton Trans.* **1988**, 2927 – 2933.

[11] C. J. Cramer, W. B. Tolman, K. H. Theopold, A. L. Rheingold, *Proc. Natl. Acad. Sci. USA* **2003**, *100*, 3635 – 3640.

[12] a) D. L. Wertz, M. F. Sisemore, M. Selke, J. Driscoll, J. S. Valentine, *J. Am. Chem. Soc.* **1998**, *120*, 5331 – 5332; b) Y. Goto, S. Wada, I. Morishima, Y. Watanabe, *J. Inorg. Biochem.* **1998**, *69*, 241 – 247; c) J. Annaraj, Y. Suh, M. S. Seo, S. O. Kim, W. Nam, *Chem. Commun.* **2005**, 4529 – 4531.

[13] a) A. D. N. Vaz, S. J. Pernecky, G. M. Raner, M. J. Coon, *Proc. Natl. Acad. Sci. USA* **1996**, *93*, 4644 – 4648; b) A. D. N. Vaz, E. S. Roberts, M. J. Coon, *J. Am. Chem. Soc.* **1991**, *113*, 5886 – 5887.

[14] a) M. S. Reynolds, A. Butler, *Inorg. Chem.* **1996**, *35*, 2378 – 2383; b) A. Butler, M. J. Clague, G. E. Meister, *Chem. Rev.* **1994**, *94*, 625 – 638.

[15] S. P. de Visser, F. Ogliaro, Z. Gross, S. Shaik, *Chem. Eur. J.* **2001**, *7*, 4954 – 4960.

